Winds of Stars and Exoplanets
Proceedings IAU Symposium No. 370, 2023
A. A. Vidotto, L. Fossati & J. S. Vink, eds.
doi:10.1017/S174392132300025X

Stellar wind from low-mass main-sequence stars: an overview of theoretical models

Munehito Shoda

Department of Earth and Planetary Science, School of Science, The University of Tokyo, 7-3-1 Hongo, Bunkyo-ku, Tokyo, 113-0033, Japan

Abstract. The stellar wind from low-mass stars affects the evolution of the whole stellar system in various ways. To better describe its quantitative contributions, we need to understand the theoretical aspects of stellar wind formation. Here, we present an overview of the theoretical models of stellar wind. The classical thermally-driven wind model fails in reproducing the anti-correlation between the coronal temperature and wind speed observed in the solar wind, thus needs modification with magnetic-energy injection. Specifically, energy input by Alfvén wave is likely to be important. Indeed, a number of solar-wind observations are well reproduced by the Alfvén-wave models, although it could be risky to directly apply the Alfvén-wave models to general low-mass stars. For a better description of stellar wind from low-mass stars with a variety of activity levels, the hybrid model would be better, in which we consider the effect of flux emergence as well as Alfvén wave.

Keywords. solar wind, stars: winds, outflows, stars: mass loss

1. Introduction

Stellar wind plays several important roles in the long-term evolution of the stellar system. For example, stellar rotational evolution in the main sequence is regulated by the angular momentum loss by the magnetized stellar wind (magnetic braking, Kraft 1967; Weber & Davis 1967; Sakurai 1985; Kawaler 1988). Stellar wind also affects the evolution of planets in the form of enhanced/suppressed atmospheric loss (Vidotto & Cleary 2020; Mitani et al. 2022) and water (hydrogen) supply (Daly et al. 2021). To better understand these processes, we need to know how the stellar-wind properties depend on the stellar fundamental parameters, such as luminosity, radius, mass, metallicity, and age (Reimers 1975; Schröder & Cuntz 2005; Cranmer & Saar 2011; Suzuki et al. 2013).

One problem underlying the stellar wind studies is the observational difficulty. Since the direct observation of the stellar wind from low-mass stars is impossible (except the solar wind), we need to infer the stellar wind parameters from model-dependent indirect methods, including the excessive absorption of the Lyman-alpha line (Wood et al. 2005, 2014, 2021), slingshot prominence (Jardine & Collier Cameron 2019), and the planetary response to the stellar wind (Vidotto & Bourrier 2017; Kavanagh et al. 2019). In spite of the various methods proposed, the number of samples is still insufficient to derive statistical properties (see Figure 8 of Vidotto 2021).

Given the observational difficulty, improving theoretical models is essential to promote our knowledge of the stellar wind. In this article, we overview the current status of the stellar-wind models. We first briefly review the classical thermally-driven wind model and its limitation. More sophisticated "magnetically-driven wind model" is discussed in the subsequent section, with a particular focus on the Alfvén-wave driven models. The summary and future prospect are given in the final section.

2. Parker's thermally-driven wind model

Motivated by the discovery of the million-kelvin envelop of the solar atmosphere (solar corona, Edlén 1943) and the double-tale structure of the comet (Biermann 1957), Parker (1958) proposed a model of the solar (and stellar) wind, which is now called the thermally-driven wind model.

2.1. *Model description*

In the thermally-driven wind model, we assume that the solar wind is described by the hydrodynamic equations. Substituting the energy equation with the polytropic equation, the governing equations of the solar wind are therefore given as follows.

$$\frac{\partial}{\partial t}\rho + \nabla\cdot(\rho\boldsymbol{v}) = 0, \tag{2.1}$$

$$\rho\frac{\partial}{\partial t}\boldsymbol{v} + \rho\left(\boldsymbol{v}\cdot\nabla\right)\boldsymbol{v} = -\nabla p - \rho\frac{GM_\odot}{r^3}\boldsymbol{r}, \tag{2.2}$$

$$\frac{\partial}{\partial t}\left(\frac{p}{\rho^\alpha}\right) + \boldsymbol{v}\cdot\nabla\left(\frac{p}{\rho^\alpha}\right) = 0, \tag{2.3}$$

where α is the polytropic index. For simplicity, we further assume the time independence and spherical symmetry, which yield

$$\frac{d}{dr}\left(\rho v_r r^2\right) = 0, \tag{2.4}$$

$$v_r\frac{dv_r}{dr} + \frac{dp}{dr} + \rho\frac{GM_\odot}{r^2} = 0, \tag{2.5}$$

$$\frac{d}{dr}\left(\frac{p}{\rho^\alpha}\right) = 0. \tag{2.6}$$

These equations are reduced to the equation of Mach number $M = v_r/c_s$ (where $c_s = \sqrt{\alpha p/\rho}$ is the sound speed) given by (Kopp & Holzer 1976)

$$\frac{M^2-1}{2M^2}\frac{dM^2}{dr} = \left[1+\left(\frac{\alpha-1}{2}\right)M^2\right]\left[\frac{2}{r} - \frac{1}{2}\left(\frac{\alpha+1}{\alpha-1}\right)\frac{GM_\odot/r^2}{E+GM_\odot/r}\right], \tag{2.7}$$

where

$$E = \frac{1}{2}v_r^2 + \frac{\alpha}{\alpha-1}\frac{p}{\rho} - \frac{GM_\odot}{r} \tag{2.8}$$

is the constant of motion (constant in r). We note that the sign of the right-hand-side of Eq. (2.7) is positive in $r < r_c$ and negative in $r > r_c$, where r_c is the critical radius given by

$$r_c = \frac{GM_\odot}{E}\frac{5-3\alpha}{4(\alpha-1)}. \tag{2.9}$$

When the corona is adiabatic ($\alpha = 5/3$), $r_c = 0$, which means that the Mach number is everywhere a decreasing function of r. Thus, the solar wind is never supersonic without non-adiabatic processes. In reality, due to thermal conduction and in-situ plasma heating, the effective value of α is smaller than 5/3, thus allowing M to increase in r.

When $\alpha < 5/3$, Eq. (2.7) has two types of solutions that exhibit the subsonic outflow in the vicinity of the Sun (Figure 1). One is the subsonic (breeze) solution that is always $M < 1$, with maximum M at $r = r_c$. The other is the transonic (wind) solution that satisfies $M = 1$ at $r = r_c$, in which M always increases in r. Given the sufficiently large pressure gap between the corona and the interstellar medium, the transonic solution is

https://doi.org/10.1017/S174392132300025X Published online by Cambridge University Press

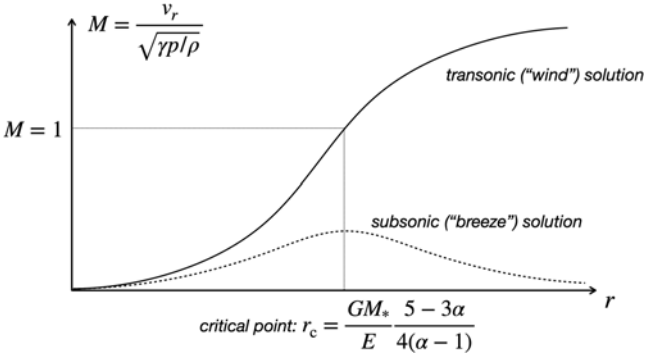

Figure 1. Mathematical solutions of the Mach-number equation Eq. (2.7) with $\alpha < 5/3$.

the only possible stationary state (Parker 1958; Velli 1994). Thus, the thermal expansion of the coronal plasma leads to the supersonic outflow.

2.2. *Limitation*

Although the thermally-driven wind model explains the emergence of the supersonic outflow as a natural consequence of coronal heating, several observations disagree with what the model predicts. For example, the solar wind is found to become slower as the coronal temperature increases, as inferred from the ionization state of the solar wind ions (Geiss et al. 1995; von Steiger et al. 2000). This is contradictory to the thermally-driven model, which predicts faster solar wind for higher coronal temperature (Parker 1958).

Another example of disagreement is the relation between the expansion factor of the solar wind and the wind speed. Fast solar wind emanates from the magnetic flux tube with a small expansion factor, and vice versa (Wang & Sheeley 1990; Arge & Pizzo 2000). According to the thermally-driven wind model, the wind tends to be faster with larger flux-tube expansion (Kopp & Holzer 1976), which is in the opposite sense to observation.

One missing physics in the thermally-driven wind model is the role of magnetic field. The solar corona is the magnetically-dominated region (Gary 2001; Iwai et al. 2014), and thus, magnetic field should dominate the energetics of the solar wind. Since the coronal thermal energy originates from the dissipation of magnetic energy (Alfvén 1947; Parker 1972, 1988; Rappazzo et al. 2008), the ideal model of the solar/stellar wind is such that solves the coronal heating and wind acceleration via the magnetic energy deposition. In the following, we call such a model "magnetically-driven wind model".

3. Magnetically-driven wind models

3.1. *Various forms of magnetic energy injection*

In the magnetically-driven wind models, we assume that the energy of the solar/stellar wind is supplied by magnetic field. Since the magnetic energy is transported via the Poynting flux, the wind models are categorized according to how the Poynting flux is generated. Under the ideal magnetohydrodynamic approximation, the vertical component of the Poynting flux is written (in cgs Gauss unit) as follows.

$$S_z = \frac{c}{4\pi}\boldsymbol{E}\times\boldsymbol{B}\Big|_z = \left(\frac{B_\perp^2}{4\pi}\right)v_z - \frac{B_z}{4\pi}\left(\boldsymbol{v}_\perp\cdot\boldsymbol{B}_\perp\right), \tag{3.1}$$

where X_z and $\boldsymbol{X}_\perp$ denote the vertical (z) and horizontal (x and y) components of $\boldsymbol{X}$, respectively.

https://doi.org/10.1017/S174392132300025X Published online by Cambridge University Press

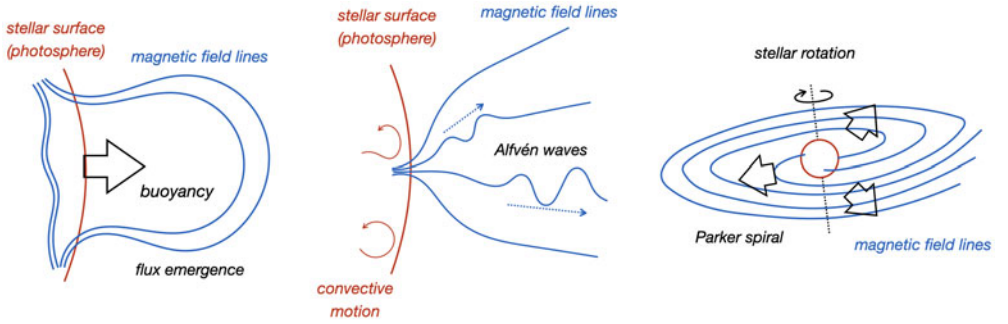

Figure 2. Various forms of Poynting-flux transport. Left: energy transport by the rising-up motion of the horizontal field (flux emergence). Center: energy transport by the transverse oscillations of the velocity and magnetic field (Alfvén wave). Right: energy transport by the magnetic rotation of the stellar wind (Parker spiral).

The first term in the right hand side of Eq. (3.1) represents the energy transfer by the rising-up motion of horizontal magnetic field, that is, flux emergence. The second term corresponds to the energy transfer by the horizontal displacements in velocity and magnetic field. Alfvén wave (Alfvén 1942) is an example of this type of energy transfer, but we note that the stellar rotation coupled with magnetic field (Parker spiral, Parker 1958; Weber & Davis 1967) also contributes to the energy transfer via the second term. The schematic images of the three processes are summarized in Figure 2.

Flux emergence, Alfvén wave and Parker spiral have different roles in the solar/stellar wind acceleration. Energy transferred by flux emergence is likely to be deposited below the critical point, because the typical height of the coronal loop is lower than the critical point. Since the energy input below the critical point leads to the increased mass flux (Hansteen & Velli 2012), the flux emergence should contribute to the larger mass-loss rate. Meanwhile, energy injection by Parker spiral occurs above the critical point, thus Parker spiral contributes to larger wind speed without increasing mass flux (Holzwarth & Jardine 2007; Shoda et al. 2020). Alfvén wave deposits energy both below and above critical points, depending on the shape of flux tube (Cranmer & van Ballegooijen 2005; Verdini & Velli 2007; Perez & Chandran 2013; Chandran & Perez 2019).

3.2. *Alfvén-wave models*

Since the effect of Alfvén wave is the easiest to incorporate in the solar wind models (using, for example, WKB approximation, Alazraki & Couturier 1971; Belcher 1971; Jacques 1977), the Alfvén-wave model is the most widely studied in the magnetically-driven wind models. It is capable of reproducing various observational aspects of the solar wind, including the radial structure of the solar wind (Suzuki & Inutsuka 2005; Cranmer et al. 2007; Verdini et al. 2010; Matsumoto & Suzuki 2012, 2014; Shoda et al. 2018, 2019; Matsumoto 2021), the anti-correlation between the flux-tube expansion and the wind speed (Suzuki & Inutsuka 2006; Cranmer et al. 2007; Shoda et al. 2022), and the global (full-sphere) structure of the solar wind (van der Holst et al. 2014; Usmanov et al. 2018; Réville et al. 2020). We show in Figure 3 the result of a direct numerical simulation of the Alfvén-wave-powered solar wind, which directly demonstrates the performance of the Alfvén-wave model.

In spite of the great performance of the Alfvén-wave model in reproducing the solar wind, it could be risky to assume that the Alfvén-wave model is applicable to any low-mass main-sequence stars. Indeed, Shoda et al. (2020) modeled the stellar wind from

https://doi.org/10.1017/S174392132300025X Published online by Cambridge University Press

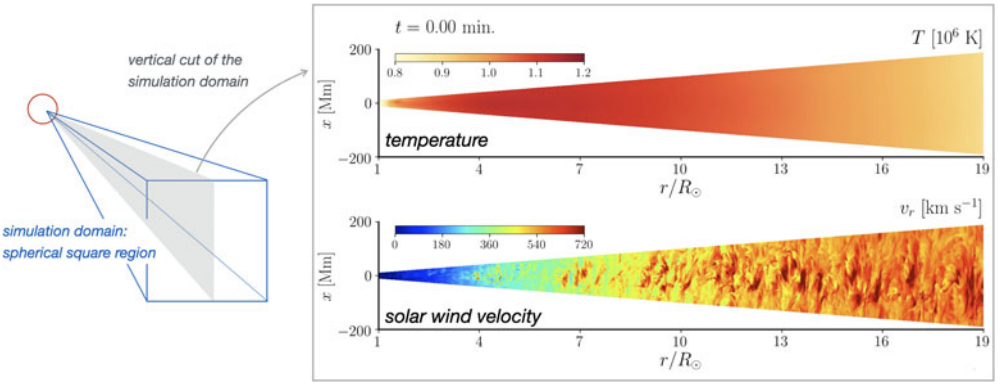

Figure 3. 3D simulation result of the solar wind based on the Alfvén-wave secario (Shoda et al. 2019). The two panels on the right show the profiles of temperature (top) and solar wind velocity (bottom) on the two-dimensional cut (indicated by the left picture).

Sun-like stars under the Alfvén-wave (+ Parker-spiral) scenario, predicting that the mass-loss rate of fast rotators is significantly smaller than the observed values (Wood et al. 2005; Jardine & Collier Cameron 2019; Vidotto 2021). Stellar wind from M-type stars are also predicted to be much weaker than observation in the Alfvén-wave models (Cranmer & Saar 2011; Sakaue & Shibata 2021). These results indicate that Alfvén waves (and Parker spiral) are insufficient to power the stellar wind from magnetically active stars.

3.3. *Flux emergence as a feeding mechanism to the stellar wind*

Flux emergence is a process in which the magnetic bundle embedded in the convection zone emerges above the surface due to magnetic buoyancy (Cheung & Isobe 2014). Flux emergence is often followed by the formation of coronal loops that exhibit large thermal and magnetic energies. Once the magnetic reconnection between the coronal loop and open field line (interchange reconnection, Crooker et al. 2002) occurs, the solar wind can be powered by the coronal-loop energy. In terms of energy flux, it means that the solar wind is accelerated by (a fraction of) energy flux carried by flux emergence. The solar wind models based on the flux emergence and interchange reconnection are called reconnection/loop-opening (RLO) models (Fisk et al. 1999; Fisk 2003; Antiochos et al. 2011; Rappazzo et al. 2012).

Although RLO models are more difficult to numerically demonstrate than Alfvén-wave models, several observations support the RLO scenario as a driving mechanism of the solar wind (Sakao et al. 2007; Harra et al. 2008; Brooks et al. 2015; Bale et al. 2022). Recent observations of magnetic switchback (Bale et al. 2019; Kasper et al. 2019) also indicate the frequent occurrence of interchange reconnection at the base of the corona (Fisk & Kasper 2020; Zank et al. 2020; Drake et al. 2021). With this background, the role of flux emergence and subsequent interchange reconnection has been attracting more interest in these years.

With the current capability of the magnetic-field observation on the Sun, the interchange reconnection is estimated to feed an insufficient amount of energy to the solar wind (Cranmer & van Ballegooijen 2010). However, the existence of small-scale coronal loops without corresponding root magnetic fields on the surface indicates that we might significantly underestimate the rate of flux emergence due to the lack of resolution, in

https://doi.org/10.1017/S174392132300025X Published online by Cambridge University Press

particular in the open-field regions (Wang 2020). Recent observations of the small-scale coronal loops (campfires, Berghmans et al. 2021) support this hypothesis.

Assuming that the rate of flux emergence in the coronal hole is the same as that in the quiet Sun, Wang (2020) estimated the energy flux by flux emergence (measured at the coronal base) as follows.

$$F^{\rm FE} \sim 2.9 \times 10^5 \left(\frac{B_0}{10\ {\rm G}}\right) \times \left(\frac{h}{6.4\ {\rm Mm}}\right) \left[\frac{E}{2.25 \times 10^{-3}\ {\rm Mx\ cm^2\ s^{-1}}}\right]\ {\rm erg\ cm^{-2}\ s^{-1}}, \tag{3.2}$$

where B_0 is the coronal magnetic field, h is the typical vertical scale of the magnetic loop, and E is the rate of flux emergence having total unsigned flux $\gtrsim 1 \times 10^{18}$ Mx. Suppose that h and E do not vary with the magnetic activity, Eq. (3.2) means that the energy flux from flux emergence is proportional to the coronal magnetic field, which is nearly equivalent to the unsigned magnetic flux on the surface. Thus, the flux emergence possibly dominates the energetics in the solar active region and magnetically active stars.

4. Summary and conclusion

In this article, we have reviewed models of the stellar wind from low-mass stars. The thermally-driven wind model naturally explains the origin of the supersonic outflow with the polytropic index $\alpha < 5/3$. Several observations show, however, qualitative disagreements with the thermally-driven wind model, thus prompting us to explicitly consider the effect of magnetic field. The Alfvén-wave model is a representative of magnetically-driven wind models, which is found to perform well in the solar wind. However, the Alfvén wave could be insufficient to power the stellar wind from magnetically-active stars, and thus, it might be necessary to consider the additional effects. Recent studies of the solar flux emergence and solar wind indicate that the flux emergence possibly playes a significant role when the magnetic activity is sufficiently strong. Our conclusion is that, to precisely model the stellar wind from stars with a range of magnetic activity, we might need a hybrid model, in which we consider both Alfvén wave and flux emergence.

Acknowledgement

Munehito Shoda is supported by a Grant-in-Aid for Scientific Research from MEXT/JSPS of Japan, 22K14077.

References

Alazraki, G. & Couturier, P. 1971, A&A, 13, 380
Alfvén, H. 1942, Nature, 150, 405
Alfvén, H. 1947, MNRAS, 107, 211
Antiochos, S. K., Mikić, Z., Titov, V. S., Lionello, R., & Linker, J. A. 2011, ApJ, 731, 112
Arge, C. N. & Pizzo, V. J. 2000, JGR, 105, 10465
Bale, S. D., Badman, S. T., Bonnell, J. W., et al. 2019, Nature, 576, 237
Bale, S. D., Drake, J. F., McManus, M. D., et al. 2022, arXiv e-prints, arXiv:2208.07932
Belcher, J. W. 1971, ApJ, 168, 509
Berghmans, D., Auchère, F., Long, D. M., et al. 2021, arXiv e-prints, arXiv:2104.03382
Biermann, L. 1957, The Observatory, 77, 109
Brooks, D. H., Ugarte-Urra, I., & Warren, H. P. 2015, Nature Communications, 6, 5947
Chandran, B. D. G. & Perez, J. C. 2019, Journal of Plasma Physics, 85, 905850409
Cheung, M. C. M. & Isobe, H. 2014, Living Reviews in Solar Physics, 11, 3
Cranmer, S. R. & Saar, S. H. 2011, ApJ, 741, 54
Cranmer, S. R. & van Ballegooijen, A. A. 2005, ApJS, 156, 265
Cranmer, S. R. & van Ballegooijen, A. A. 2010, ApJ, 720, 824

https://doi.org/10.1017/S174392132300025X Published online by Cambridge University Press

Cranmer, S. R., van Ballegooijen, A. A., & Edgar, R. J. 2007, ApJS, 171, 520
Crooker, N. U., Gosling, J. T., & Kahler, S. W. 2002, Journal of Geophysical Research (Space Physics), 107, 1028
Daly, L., Lee, M. R., Hallis, L. J., et al. 2021, Nature Astronomy, 5, 1275
Drake, J. F., Agapitov, O., Swisdak, M., et al. 2021, A&A, 650, A2
Edlén, B. 1943, ZA, 22, 30
Fisk, L. A. 2003, Journal of Geophysical Research (Space Physics), 108, 1157
Fisk, L. A. & Kasper, J. C. 2020, ApJ Letters, 894, L4
Fisk, L. A., Schwadron, N. A., & Zurbuchen, T. H. 1999, JGR, 104, 19765
Gary, G. A. 2001, Solar Physics, 203, 71
Geiss, J., Gloeckler, G., & von Steiger, R. 1995, Space Science Reviews, 72, 49
Hansteen, V. H. & Velli, M. 2012, Space Science Reviews, 172, 89
Harra, L. K., Sakao, T., Mandrini, C. H., et al. 2008, ApJ Letters, 676, L147
Holzwarth, V. & Jardine, M. 2007, A&A, 463, 11
Iwai, K., Shibasaki, K., Nozawa, S., et al. 2014, Earth, Planets and Space, 66, 149
Jacques, S. A. 1977, ApJ, 215, 942
Jardine, M. & Collier Cameron, A. 2019, MNRAS, 482, 2853
Kasper, J. C., Bale, S. D., Belcher, J. W., et al. 2019, Nature, 576, 228
Kavanagh, R. D., Vidotto, A. A., Ó. Fionnagáin, D., et al. 2019, MNRAS, 485, 4529
Kawaler, S. D. 1988, ApJ, 333, 236
Kopp, R. A. & Holzer, T. E. 1976, Solar Physics, 49, 43
Kraft, R. P. 1967, ApJ, 150, 551
Matsumoto, T. 2021, MNRAS, 500, 4779
Matsumoto, T. & Suzuki, T. K. 2012, ApJ, 749, 8
Matsumoto, T. & Suzuki, T. K. 2014, MNRAS, 440, 971
Mitani, H., Nakatani, R., & Yoshida, N. 2022, MNRAS, 512, 855
Parker, E. N. 1958, ApJ, 128, 664
Parker, E. N. 1972, ApJ, 174, 499
Parker, E. N. 1988, ApJ, 330, 474
Perez, J. C. & Chandran, B. D. G. 2013, ApJ, 776, 124
Rappazzo, A. F., Matthaeus, W. H., Ruffolo, D., Servidio, S., & Velli, M. 2012, ApJ Letters, 758, L14
Rappazzo, A. F., Velli, M., Einaudi, G., & Dahlburg, R. B. 2008, ApJ, 677, 1348
Reimers, D. 1975, Memoires of the Societe Royale des Sciences de Liege, 8, 369
Réville, V., Velli, M., Panasenco, O., et al. 2020, ApJS, 246, 24
Sakao, T., Kano, R., Narukage, N., et al. 2007, Science, 318, 1585
Sakaue, T. & Shibata, K. 2021, ApJ, 919, 29
Sakurai, T. 1985, A&A, 152, 121
Schröder, K. P. & Cuntz, M. 2005, ApJ Letters, 630, L73
Shoda, M., Iwai, K., & Shiota, D. 2022, ApJ, 928, 130
Shoda, M., Suzuki, T. K., Asgari-Targhi, M., & Yokoyama, T. 2019, ApJ Letters, 880, L2
Shoda, M., Suzuki, T. K., Matt, S. P., et al. 2020, ApJ, 896, 123
Shoda, M., Yokoyama, T., & Suzuki, T. K. 2018, ApJ, 853, 190
Suzuki, T. K., Imada, S., Kataoka, R., et al. 2013, PASJ, 65, 98
Suzuki, T. K. & Inutsuka, S.-i. 2005, ApJ Letters, 632, L49
Suzuki, T. K. & Inutsuka, S.-I. 2006, Journal of Geophysical Research (Space Physics), 111, A06101
Usmanov, A. V., Matthaeus, W. H., Goldstein, M. L., & Chhiber, R. 2018, ApJ, 865, 25
van der Holst, B., Sokolov, I. V., Meng, X., et al. 2014, ApJ, 782, 81
Velli, M. 1994, ApJ Letters, 432, L55
Verdini, A. & Velli, M. 2007, ApJ, 662, 669
Verdini, A., Velli, M., Matthaeus, W. H., Oughton, S., & Dmitruk, P. 2010, ApJ Letters, 708, L116
Vidotto, A. A. 2021, Living Reviews in Solar Physics, 18, 3

Vidotto, A. A. & Bourrier, V. 2017, MNRAS, 470, 4026
Vidotto, A. A. & Cleary, A. 2020, MNRAS, 494, 2417
von Steiger, R., Schwadron, N. A., Fisk, L. A., et al. 2000, JGR, 105, 27217
Wang, Y. M. 2020, ApJ, 904, 199
Wang, Y. M. & Sheeley, N. R., J. 1990, ApJ, 355, 726
Weber, E. J. & Davis, Leverett, J. 1967, ApJ, 148, 217
Wood, B. E., Müller, H.-R., Redfield, S., & Edelman, E. 2014, ApJ Letters, 781, L33
Wood, B. E., Müller, H.-R., Redfield, S., et al. 2021, ApJ, 915, 37
Wood, B. E., Müller, H. R., Zank, G. P., Linsky, J. L., & Redfield, S. 2005, ApJ Letters, 628, L143
Zank, G. P., Nakanotani, M., Zhao, L. L., Adhikari, L., & Kasper, J. 2020, ApJ, 903, 1

https://doi.org/10.1017/S174392132300025X Published online by Cambridge University Press